BIOCHEMISTRY
including biophysical chemistry & molecular biology
Article

Biochemistry **2010,** *49,* 7847–7853 7847
DOI: 10.1021/bi1006833

Polyhistidine Peptide Inhibitor of the Aβ Calcium Channel Potently Blocks the Aβ-Induced Calcium Response in Cells. Theoretical Modeling Suggests a Cooperative Binding Process†

Nelson Arispe,*,‡ Juan Diaz,‡ Stewart R. Durell,§ Yinon Shafrir,§ and H. Robert Guy*,§

‡*Department of Anatomy, Physiology and Genetics, Uniformed Services University of the Health Sciences, Bethesda, Maryland 20814, and* §*Laboratory of Cell Biology, National Cancer Institute, National Institutes of Health, Bethesda, Maryland 20892*

Received May 3, 2010; Revised Manuscript Received July 9, 2010

ABSTRACT: On the basis of the consistent demonstrations that the Aβ peptide of Alzheimer's disease forms calcium permeant channels in artificial membranes, we have proposed that the intracellular calcium increase observed in cells exposed to Aβ is initiated by calcium fluxes through Aβ channels. We have found that a small four-histidine peptide, NAHis04, potently inhibits the Aβ-induced calcium channel currents in artificial lipid membranes. Here we report that NaHis04 also potently blocks the intracellular calcium increase which is observed in cells exposed to Aβ. PC12 cells loaded with Fura-2AM show a rapid increase in fluorescence and a rapid return to baseline after Aβ is added to the medium. This fluorescence change occurs even when the medium contains nitrendipine, a voltage-gated calcium channel blocker, but fails to occur when application of Aβ is preceded by addition of NAHis04. Steep dose−response curves of the percentage of responding cells and cell viability show that NAHis04 inhibits in the micromolar range in an apparently cooperative manner. We have developed numerous models of Aβ pores in which the first part of the Aβ sequence forms a large β-barrel ending at His 13. We have modeled how up to four NAHis04 peptides may block these types of pores by binding to side chains of Aβ residues Glu 11, His 13, and His 14.

The Aβ peptide of Alzheimer's disease has been shown to form calcium permeant channels in artificial and natural membranes (refs *1* and *2*; for a review, see ref *3*). We have proposed that cytotoxic action of Aβ is due to an intracellular calcium increase initiated by calcium fluxes across the cell membrane through Aβ channels (*3*−*5*). With the hope of developing treatments for Alzheimer's disease, we have modeled the structure of the Aβ channels and are attempting to design effective blocker compounds endowed with therapeutic potential. Early theoretical models (*6*) proposed that the N-terminal region (residues 1−14) forms the lining of the Aβ channel's pore. This region was selected because negatively charged residues at positions 1, 3, 7, and 11 can account for the experimentally observed cation selectivity of the channel and because the presence of histidines at positions 6, 13, and 14 can account for experimentally observed blockade of the channels by Zn^{2+} (*2*, *7*) and Al^{3+} (*1*). This concept has been retained in a new generation of models that are consistent with microscopy studies (*8*). A series of small peptides that copy the sequence of segments of this region of the Aβ molecule have been found to effectively interfere with ion flow across the Aβ channels formed in lipid membranes (*9*, *10*), as long as they contain histidine residues at positions analogous to H13 and H14. The importance of histidines in the inhibition process is strengthened by the finding that polyhistidine peptides are also potent inhibitors of Aβ-induced calcium channel currents in artificial lipid membranes (*11*). Additionally, these compounds have also been found to prevent Aβ cytotoxicity (*10*−*12*). Here we report that one of these peptides, NaHis04, also potently blocks the intracellular calcium increase that is observed in cells exposed to Aβ. Steep dose−response curves of the percentage of cells that respond with an intracellular calcium increase upon exposure to Aβ, and the viability of cells studied in the presence of NAHis04, show that inhibitions occur in the micromolar range in an apparently cooperative manner. We also show that in theoretical molecular models of Aβ pores in which residues 1−13 form a large β-barrel lined with charged and polar−neutral residues, multiple NAHis04 peptides may block the pore by binding in a cooperative manner to the side chains of Aβ residues Glu 11, His 13, and His 14. This theoretical finding is in good agreement with the experimental results obtained with NaHis04.

METHODS

Planar Lipid Bilayer. The methodology followed here has been described previously (*1*, *11*). Briefly, to form lipid bilayers, a 1:1 suspension of palmitoyloleoylphosphatidylserine and palmitoyloleoylphosphatidylethanolamine (Avanti) in *n*-decane was applied to an orifice in a TeflonTM film separating two compartments. The ionic solutions in the compartments contained asymmetrical concentrations of CsCl (200 mM cis/50 mM trans) and symmetrical 0.5 mM $CaCl_2$ and 5 mM K-HEPES (pH 7). The current between the two compartments was recorded using a patch clamp amplifier in V-clamp mode, and data were stored on a computer disk. Off-line analysis of the channel activity was

†This work was supported by grants from The Alzheimer's Association of America and The Uniformed Services University of the Health Sciences.

*To whom correspondence should be addressed. N.A.: Department of Anatomy, Physiology and Genetics, Uniformed Services University of the Health Sciences, 4301 Jones Bridge Rd., Bethesda, MD 20814; telephone, (301) 295-9367; fax, (301) 295-1715; e-mail, narispe@usuhs.mil. H.R.G.: 6510 Tahawash St., Cochiti Lake, NM 87083; telephone, (505) 465-2445 or (301) 767-5455; fax, (301) 402-4724; e-mail, bg4y@nih.gov or guyh@exchange.nih.gov.

Published on Web 08/06/2010

conducted using pClamp (Axon Instruments, Foster City, CA). Incorporation of the Aβ peptide into the bilayer was achieved via addition of an aliquot of a proteoliposome (Aβ40 liposome) suspension to the solution on the cis side of the planar lipid bilayer chamber and stirring.

Preparation of Proteoliposomes. We prepared proteoliposomes (Aβ40 liposomes) by mixing a liposome suspension with a stock aqueous solution of Aβ40 peptide (1 mg/mL) followed by sonication. Liposomes were prepared by hydration of air-dried palmitoyloleoylphosphatidylserine (10 mg) with 1 M potassium aspartate (pH 7.0, 1 mL), followed by water sonication for 5 min.

Cell Culture. PC12 cells, derived from a transplantable rat pheochromocytoma (ATCC # CRL 1721), were cultured in the recommended ATCC medium. Primary cultures of hippocampal and cortical neurons from P18−P21 rat brains were grown in neurobasal medium/B27 (GIBCO). For neuron preparation, pregnant rats were anesthetized and sacrificed to extract the fetuses. For pain alleviation, the animals were anesthetized following recommendations on 2000 Report of the AVMA (American Veterinary Medical Association) Panel on Euthanasia. Brains from the fetuses were dissected and neuronal cell cultures prepared as in a previously described protocol (*10*, *12*).

Intracellular Free Calcium Measurements. PC12 cells were cultured for a minimum of 24 h via adhesion on glass coverslips coated with collagen or polylysine. In a coverslip holding chamber, cells were loaded with 5 μM FURA-2AM (Molecular Probes) calcium-sensitive probe in 300 μL of incubation medium. After a loading period (approximately 30 min), the incubation medium was changed to 300 μL of a buffer solution [135 mM NaCl, 5 mM KCl, 2.5 mM $CaCl_2$, 1.2 mM $MgCl_2$, 10 mM glucose, and mM 10 Hepes (pH 7.4)]. The time course of changes in the emission from Fura-2AM was observed using an inverted epi-fluorescence/phase contrast microscope equipped with a CCD camera and microphotometer assembly (InCyt I/P-2 Imaging & Photometry System, Intracellular Imaging). Cells were exposed to either Aβ40 or Aβ42 via addition of small aliquots (0.7 μL) of Aβ (final concentration of 0.5 μM) to the 300 μL buffer solution of the coverslip holding chamber. The emissions from 40−60 cells were simultaneously recorded in each experiment.

Cell Viability Assays. The percentage of cells protected by the Aβ channel inhibitor from the Aβ40-induced cell death was evaluated by a colorimetric XTT assay (Cell Proliferation Kit II, Roche).

Materials. Aβ was purchased from Biosource, AnaSpec, and Peptides International as Aβ40 and dissolved in either water or DMSO following the manufacturer's suggestion. NAHIS04 was synthesized in the Biomedical Instrumentation Center at the Uniformed Services University of the Health Sciences utilizing an Applied Biosystems model 433A peptide synthesizer. The chemistry used to produce NAHIS04 was the HBTU/DIEA activation of Fmoc amino acids as an amide and capped at the amino terminus with acetic anhydride.

Molecular Modeling. We used AutoDoc4 to dock single-peptide blocker NAHIS04 into the central region of a previously developed model of the Aβ channel. In this model, we assigned positive charges to two of the four histidine side chains that form the NAHIS04 molecule. In the Aβ channel model, we charged half of the His 13 side chains and none of the more buried His 14 side chains. Due to the symmetry of the channel modeled, the central pore region has 12 equivalent binding sites. We noticed that at least one blocker peptide could be added in all of the channel models and that in three cases three more blocker peptides could be added, with some small adjustments using energy minimization to eliminate bad contacts and improve good ones. We used one of these to develop the model illustrated in Figure 4 containing four NaHIS04 peptides. This model was minimized with 2-fold symmetry about the axis of the pore and 2-fold symmetry about the central plane of the membrane to produce the final model in which all NaHIS04 peptides have identical conformations and interactions with the channel.

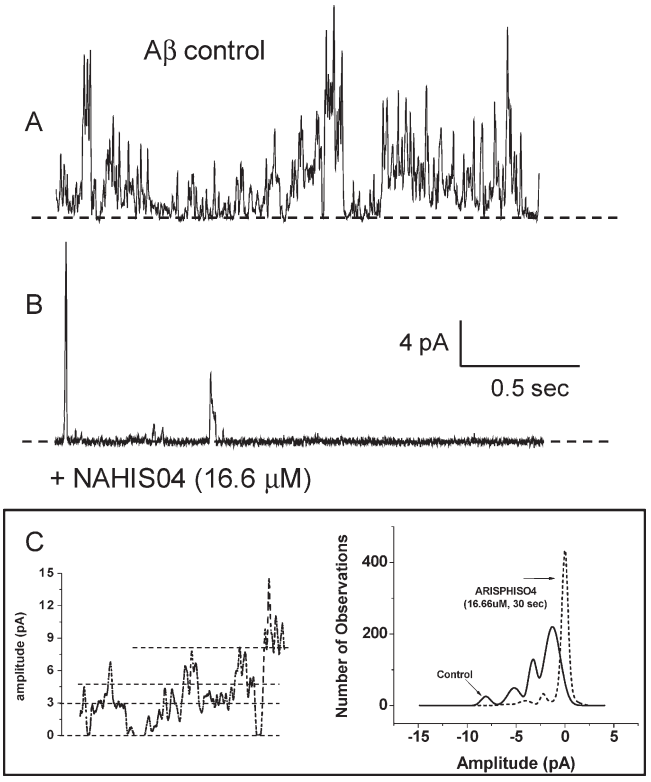

FIGURE 1: NAHIS04 irreversibly blocks the membrane-bound Aβ ion channel. (A) Characteristic electrical activity across incorporated Aβ channels (control). The electrical potential of the bilayer is maintained at zero, and the ionic current across the Aβ channel is driven uniquely by a chemical gradient. The Aβ channel operates between multiple conductance levels. (B) After NAHIS04 is added to the solution bathing the bilayer, the electrical activity stops, suggesting a full block of the channel. Panel C displays a time expanded segment of the electrical record to indicate (···) well-defined current levels of three discrete jumps of current. At the right, the current amplitude histograms assemble the channel activity from the current traces in panels A and B. Four main current peaks of 1.7, 3, 5.2, and 8.5 pA characterize the Aβ channel activity. NAHIS04 quickly abolishes the most frequent current peaks.

RESULTS

NAHIS04 Blocks the Ionic Currents through Aβ Channels Incorporated in Lipid Bilayers. Before we attempt to prevent the effect of Aβ ion channels on cells by using Aβ channel inhibitors, it is useful to confirm that the proposed blocker be effective at blocking the Aβ channels in a much simpler artificial system. Planar lipid bilayers were exposed to Aβ, and the inhibitor was studied after the incorporation and formation of Aβ channels. Here we used a polyhistidine compound, NAHIS04, that we have previously shown to be a selective Aβ channel inhibitor (*10*). The typical current activity from Aβ channels incorporated into a lipid bilayer is illustrated in the current records displayed in Figure 1. The electrical potential of the bilayer is maintained at zero, and the ionic current across the Aβ channel is driven uniquely by a

chemical gradient to minimize the effects of additional forces imposed on membrane-incorporated Aβ molecules. Current recordings from an Aβ channel displayed in panel A illustrate that Aβ channels operate between multiple conductance levels, which has been described previously (*1*, *12*). Several seconds after the channel was exposed to the compound NAHIS04, at a concentration of 16.6 μM, the current peaks disappeared from the record, indicating that the channel conductance was completely inhibited (panel B).

Figure 1C illustrates the multiple-conductance nature of the channel conductance. The figure of a time expanded segment of the current record shows discrete jumps of current to different well-defined levels, as marked by the dotted line. The amplitude histograms of all the current events during a time interval of 8 min of channel activity, at the right side of panel C, show all defined current peaks and correspond to the channel activity before and after the addition of NAHIS04. The addition of NAHIS04 quickly (30 s) eliminates the most frequent peak current values (3, 5.2, and 8.5 pA).

NAHIS04 Inhibits the Intracellular Calcium Increase Observed When Cells Are Exposed to Aβ. We have proposed that the intracellular calcium increase observed when cells are exposed to Aβ is initiated by calcium ions flowing across the membrane through newly formed Aβ calcium channels (*4*, *12*). To experimentally test this proposal, we studied the intracellular calcium response induced by Aβ40 and Aβ42 on PC12 cells and examined the results of using NAHIS04, which effectively inhibits Aβ-induced currents in artificial membranes. PC12 cells were grown on a coverslip, loaded with the calcium-sensitive probe Fura-2AM, and observed with the calcium imaging system. Cells were consecutively exposed to Aβ by local applications of aliquots of solutions containing Aβ. To allow the natural conversion of Aβ into the ion channel-forming species, we applied Aβ from freshly prepared solutions. The time course of changes in the emission from Fura-2AM was recorded before and up to 30 min after the Aβ applications; 50−60 cells at different positions of the optical field were analyzed under each experimental condition. The records in Figure 2 show cellular calcium responses to two consecutive local applications, at the time indicated by the arrows, of aliquots (0.7 μL) of Aβ40 and Aβ42 (final concentration of 0.5 μM). Each application of Aβ triggers an immediate transitory intracellular calcium increase, which is rapidly buffered by the cell. We failed to see any measurable Aβ-induced intracellular calcium increase when cells were studied in Ca^{2+}-free medium (not shown). This result is consistent with preceding observations that have established the external calcium dependence of this event (*13*−*16*). The records in panels A and B show the cellular calcium responses to two consecutive applications of Aβ42 and Aβ40, respectively. The calcium peaks observed after the first application of Aβ demonstrate that cells are similarly responsive to either Aβ40 or Aβ42; however, in the presence of 10 μM NAHIS04, the calcium responses after the second Aβ applications were not observed. The records in panel A are averaged records of the response from selected cells, which showed similar responses to Aβ42. Although we observed variations in the magnitude and the time course in the calcium response of different cells, we selected cells that exhibited similar responses to present an averaged response representative of our findings. Of all cells recorded (n = 31), 100% of the cells responded positively to the application of Aβ42, and all showed absolute inhibition of the intracellular Ca^{2+} increase by NAHIS04. The mean amplitude of the calcium change induced by Aβ42 was 139.97 ± 79.69 (standard deviation).

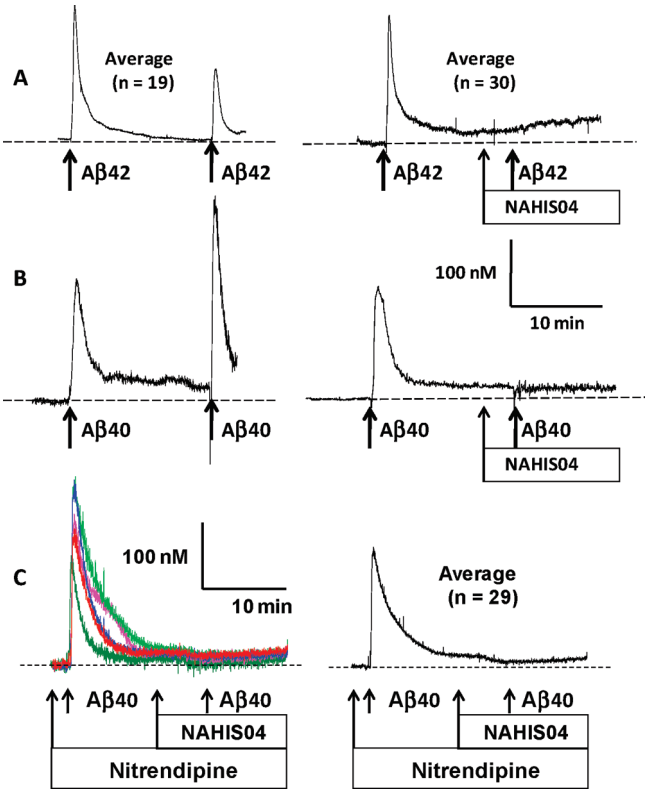

FIGURE 2: NAHIS04 inhibits the Aβ40- and Aβ42-induced calcium response. Cellular calcium responses elicited by PC12 cells loaded with Fura-2AM, after consecutive local applications (arrows) of aliquots (0.7 μL) of either Aβ42 (0.5 μM) or Aβ40 (0.5 μM). (A) Averaged record (n = 19) from control cells (left) and averaged record (n = 30) from cells treated with NAHIS04 (10 μM) before the second application of Aβ42 (right). (B) Single records from a control cell (left) and from a cell treated with NAHIS04 (10 μM) before the second application of Aβ40 (right). (C) Superimposed records from five different cells that received local applications of Aβ40 (0.5 μM) (arrows) while in the presence of nitrendipine (10 μM) (left). Nitrendipine does not prevent the calcium responses elicited by Aβ. However, no calcium response is observed when NAHIS04 is added before the second application of Aβ40. The right panel shows an average record from 29 cells subjected to the same protocol.

The records in panel B show the cellular calcium responses of two single cells to two consecutive Aβ40 applications. The record on the right side of the panel shows the response to Aβ when the channel blocker NAHIS04 was applied prior to the second application of Aβ40. Panel C (left) display simultaneous records from five representative cells responding to Aβ40. In this experiment, the applications of Aβ40 were preceded by the addition of 10 μL of nitrendipine (final concentration of 33 μM) to the buffer solution. Nitrendipine, commonly used to block voltage-dependent calcium channels, does not inhibit the calcium response from the cells. On the other hand, application of the specific Aβ channel blocker, NAHIS04, just before the second application of Aβ40 was very effective in preventing an intracellular calcium response. The record in panel C (right) is an averaged record of the response from 37 selected cells, which showed similar responses to Aβ40 with the same experimental protocol. In this experiment, of all cells recorded (n = 57), 92% of the cells responded positively to the application of Aβ40 and all but one showed absolute inhibition of the intracellular Ca^{2+} increase by NAHIS04. The mean resting calcium level of PC12 cells was 106.27 ± 5.27 (standard deviation) nM, and the mean amplitude of the calcium change induced by Aβ40 was 174 ± 49.46 (standard deviation).

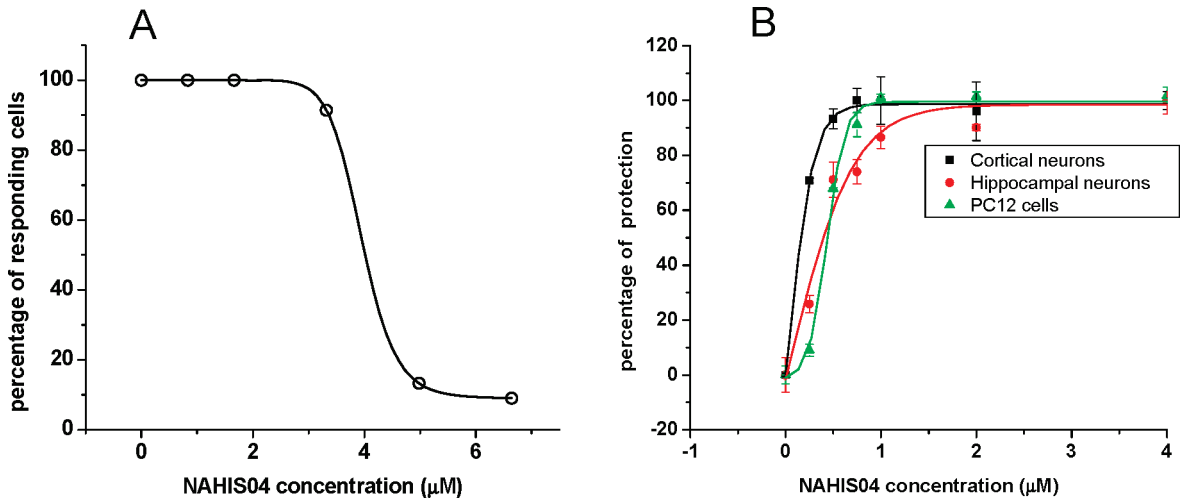

FIGURE 3: NAHIS04 inhibits the Aβ-induced calcium response and protects cells and neurons in a concentration-dependent manner. (A) Effect of NAHIS04 concentration on the percentage of cells responding with an intracellular calcium concentration change upon addition of Aβ40 (7.66 μM). (B) Steep dose−response curves to evaluate the protection of NAHIS04, added to the cell culture medium, on PC12 cells and cortical and hippocampal neurons during prolonged exposure to Aβ40 (5 μM). The viability of the three types of cells, after incubation for 3 days in the presence of Aβ40 peptide, was measured with the XTT assay and is expressed as the percentage of viable cells with respect to control. The dose−/response fit to the data produced p values of 12.96267 ± 0.00062 for the curve in panel A and 4.65205 ± 0.75189, 1.3094 ± 0.50985, and 3.39025 ± 1.02216 for the curves in panel B for PC12 cells and hippocampal and cortical neurons, respectively. The results of both experimental protocols show that there seems to be a logistical protection by NAHIS04 of the cellular effects produced by Aβ.

The averaged record shows that the inability of nitrendipine to affect the calcium response and the ability of NAHIS04 to completely inhibit the response are very consistent observations. These findings strongly support the participation of Aβ channels in the generation of the cellular calcium response.

NAHIS04 Inhibition of the Effect of Aβ on Cells Suggests a Cooperative Mechanism. We observed here that the magnitude of the calcium response induced by Aβ varies within a wide range. In the experiment illustrated in Figure 2C, the calcium change in the cells responding to the application of Aβ varied between a minimum of 97 nM and a maximum of 277 nM, from the mean resting level. It has been shown elsewhere that the magnitude and time course of the calcium response to Aβ depend on a series of factors, such as the type of cell, the concentration, and the time of application of Aβ (*12*, *17*). With freshly prepared Aβ, we have also observed that the effectiveness in blocking the variable Aβ-induced calcium response and the cytotoxicity of Aβ also critically depend on other factors such as the concentration of the inhibitor. To further analyze these observations, we compiled data from a series of experiments in which the conditions of the Aβ insult, such as the Aβ concentration and the time of application of both Aβ and NAHIS04, were kept constant, while we studied the effect of different concentrations of NAHIS04. Figure 3 show the results in terms of the percentage of cells responding with an intracellular calcium concentration change upon addition of Aβ (panel A) and the percentage of cells that remain viable during prolonged exposure to Aβ (panel B) plotted as a function of NAHIS04 concentration. The data shown in panel A were obtained from PC12 cells grown on a coverslip and loaded with the calcium-sensitive probe Fura-2AM. Cells were exposed to Aβ by a local application of an aliquot of an Aβ-containing solution; 50−60 cells at different positions of the optical field were analyzed under each experimental condition. Each point in the curve shown in panel A corresponds to an individual experiment in which the calcium image of each cell was recorded before and after the addition of Aβ. The number of cells analyzed in each individual experiment varied according to the cell density of the optic field, and the value plotted is the percentage of cells responding to Aβ. The percentage of cell protection by NAHIS04 during prolonged exposure of cells to Aβ, shown in panel B, was determined by detecting the viable cells with a colorimetric XTT assay, after incubation for 3 days of cells in medium containing Aβ (5 μM) and various concentrations of NAHIS04. The results plotted in this panel compile the results obtained from PC12 cells and ex vivo cultures, and rat cortical and hippocampal neurons. The results from the two different experimental protocols compiled in the two panels of this figure, although very different in nature, produced results that for different concentrations of the blocker can be appropriately fitted with a sigmoid function. The logistic fit to the data displayed in the two plots suggests a cooperative action on the responses, as the p value for the curve in panel A is 12.962 ± 0.0006 and the p values for the curve in panel B are 4.65205 ± 0.75189 for PC12 cells and 1.3094 ± 0.50985 and 3.39025 ± 1.02216 for hippocampal and cortical neurons, respectively. This behavior may be due to variability in the numbers of Aβ channels in the surface membrane of each cell and/or the participation of more than one channel blocker molecule in the channel blocking process.

Modeling the Binding of NAHIS04 to Aβ Channels. It has been suggested that interactions among the side chains in the histidine-containing inhibitors, and His residues in the Aβ channels, constitute a blocking mechanism for the Aβ-induced current flow across artificial membranes and for protecting cells from Aβ toxicity (*11*). Our experimental data show a cooperative mechanism for inhibition of the Aβ channels by NAHIS04, suggesting the possible participation of more than one inhibitor molecule in these processes. We studied the feasibility of this mechanism, and the way that NAHIS04 molecule and Aβ channel interactions may occur, by modeling interactions of NAHIS04 peptides with theoretical models of the Aβ channels. We have developed scores of alternative models of Aβ channels. For this study, we used the model most consistent with our modeling criteria (e.g, almost all hydrophobic groups are buried or exposed to lipid alkyl chains, almost all polar atoms form hydrogen bonds or are exposed to

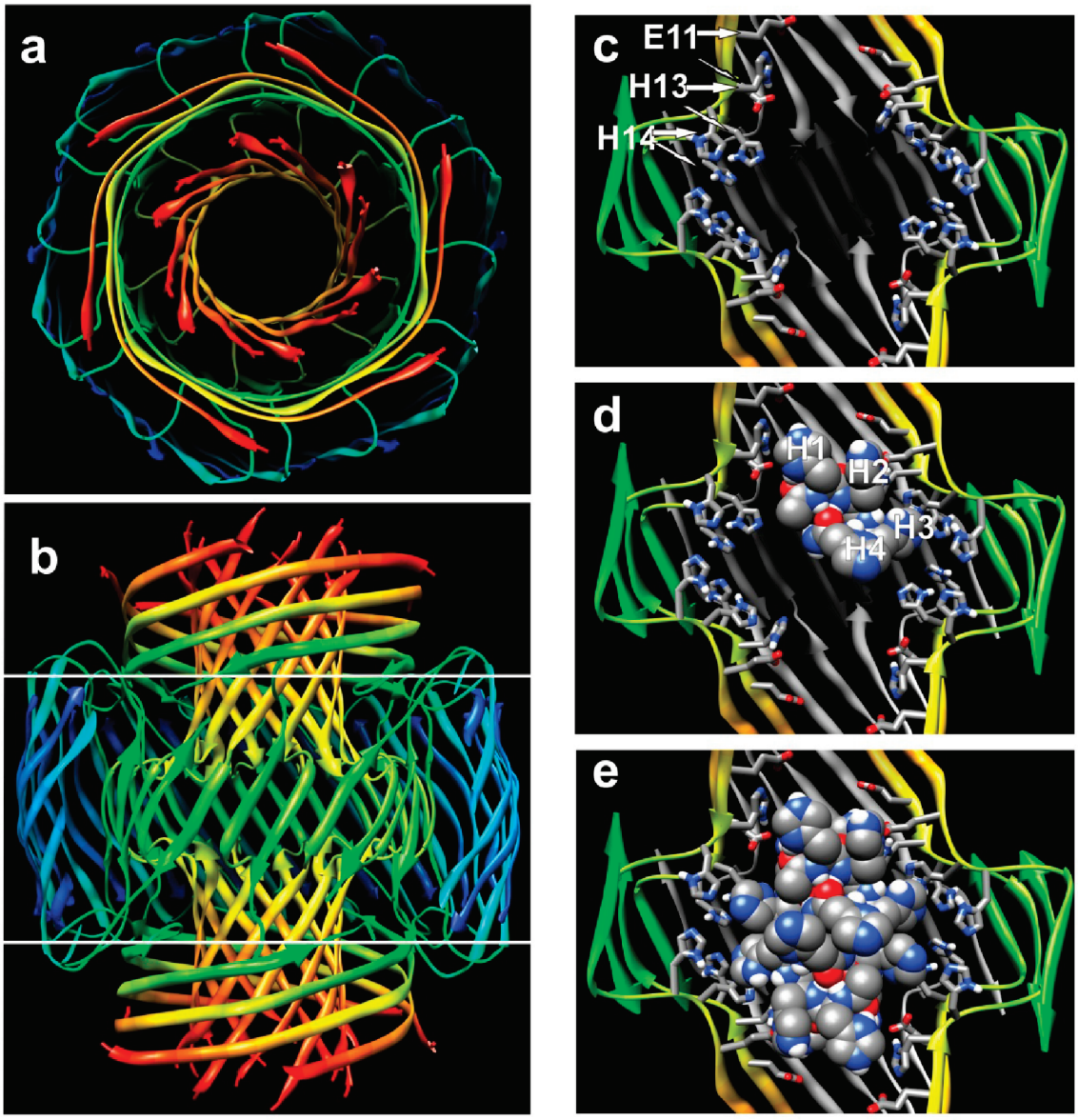

FIGURE 4: Models of the Aβ channel and its blockade by NAHIS04 peptides. (a and b) Ribbon representation of the channel model colored by the spectrum beginning with red N-termini and ending with blue C-termini. (a) Half of the structure viewed from the aqueous phase through the central pore. (b) Side view of the entire structure. The white lines approximate the boundary of the membrane's alkyl phase. (c) Enlarged side view of the central portion of the pore showing E11, H13, and H14 side chains that form the putative central drug and peptide binding site. For the sake of simplicity, subunits nearest the viewer were removed and those on the far side were colored gray; side chains are shown for only four spectrum-colored subunits on the sides of the assembly. (d and e) Same as panel c but with one (d) and four (e) space-filled NAHIS04 blocking peptides shown. Side chains and NAHIS04 are colored by element: red for O, blue for N, gray for C, and white for H.

water, almost all charged groups form salt bridges or bind to counterions in the pore, and the model is very stable during molecular dynamics simulations) that is also consistent with a preponderance of experimental results [microscopy images (*18*), selectivity of the pore for cations, and permeability to Ca^{2+} (*1*) inhibition of Aβ-induced currents by Zn^{2+} (*2*, *7*), Al^{3+} (*1*), and positively charged organic drugs, MRS2481 and MRS 2485 (*19*)]. Details of this model have been presented elsewhere (*8*). Here we concentrate on how NAHIS04 may bind to this and similar structures. Figure 4 displays this model and illustrates one way multiple NAHIS04 peptides could bind. Panels a and b show ribbon representations of the entire channel model viewed from the top (a) and side (b). The 36-subunit structure has 6-fold symmetry about the axis of the pore and 2-fold symmetry relative to the central plane of the membrane. Residues are colored by the spectrum beginning with red and ending in blue. The assembly contains 12 copies of three subunit conformational types, which we call Sub_1, Sub_2, and Sub_3. Blue-colored residues 29−42 form similar β-strands in all subunits, and these strands form a 36-strand antiparallel β-barrel that surrounds the transmembrane region. All residues of these segments are either hydrophobic or glycine. The red-colored N-termini of all subunits extend from the aqueous phases into the transmembrane region on each side of the membrane. Sub_1 and Sub_2 have similar conformations in which residues 7−25 span the bilayer and are positioned inside the 36-strand β-barrel. Residues 1−13 of these subunits form a 12-strand parallel β-barrel on each end of the assembly, and these meet near the central plane of the membrane. Green-colored hydrophobic residues 17−21 of these subunits form a centrally located 24-strand antiparallel β-barrel. Residues 1−22 of Sub_3 form a long curved β-strand that surrounds the 12-strand β-barrels on each side. Residues 1−29 of Sub_3 and residues 1−5 and 23−29 of Sub_1 and

Sub_2, respectively, are the most speculative, most water-exposed, and most dynamic parts of the model, but they are not involved in forming the putative NAHIS04 binding site.

Figure 4c illustrates a side view of the central portion of an Aβ channel model formed by the segments from E11 through A21 of the Sub_1 and Sub_2 subunits. Subunits that would be in front are not shown, and subunits on the back side are colored gray and have no side chain shown. Twenty-four H13 and 24 H14 residues comprise the lining of the central region. This region is flanked on each side by rings of negatively charged E11 side chains (12 on each side). Panel d illustrates a NAHIS04 peptide bound in this region, and panel e illustrates four bound NaHIS04 peptides; the blocking peptides all have the same conformation and are related by 2-fold symmetry about the *y*-axis and 2-fold symmetry about the *x*-axis. His 1 and His 2 side chains of NAHIS04 peptides were positively charged in this model and bind to negatively charged E11 side chains of the channel. His 3 and His 4 side chains of NAHIS04 were not charged and interact with H13 and H14 side chains of the channel and with their counterparts in other NAHIS04 peptides. The methods and rationale used to develop this model are described in Methods. However, it is important to realize that this is not a unique model for binding of NAHIS04 to Aβ channels; there are other ways to fit four blocking peptides in the channel with these symmetry constraints, many more ways if blocking peptides do not have identical conformations and are not related by symmetry, and many more ways to fit fewer than four peptides into the pore. Also, the charges of the histidine side chains are difficult to predict and will likely fluctuate with time, so this model should be considered a simple illustration of one of many ways that the peptides could block the channel by interacting with the E11, H13, and H14 side chains of the pore. This lack of uniqueness is actually energetically favorable from the entropic point of view, but it does make it difficult to predict exactly how the block occurs or to calculate the binding energy and/or binding constant. The major point is that β-barrel models of Aβ pores that include residues E11−H13 can have a pore sufficiently large to accommodate multiple NaHIS04 peptides, and that the four imidazole rings of each of the blocking peptides can interact in an energetically favorable manner with the E11 carboxyls and/or imidazole rings of the His 13 and His 14 residues of the pore.

DISCUSSION

One of the possible mechanisms by which NAHIS04 may block the conductance of the Aβ channels is by an interaction between NAHIS04 molecules and the region of the Aβ channel lining of the pore, thus interfering with the ions flowing through the channel. In cells exposed to Aβ, the interaction of Aβ with the plasma membrane results in elevated intracellular (cytoplasmic) Ca^{2+} concentrations, which is known as the Aβ-induced cellular calcium response (*13*). This response is due primarily to calcium released from intracellular calcium stores and entry of calcium from the extracellular medium (*20*−*22*). It has been previously shown that the neurotoxicity caused by Aβ does not occur in calcium-deficient culture medium (*13*), and Aβ-induced changes in cell morphology and Ca oscillation in response to Aβ are not observed when cells are incubated in a nominally Ca free medium (*14*−*16*). According to our proposed mechanisms for the Aβ induction of the cellular calcium response (*4*, *5*), extracellular calcium enters through the newly formed Aβ channels, inducing additional release of calcium from intracellular stores. Therefore, the blockage of Aβ channels by NAHIS04 should prevent the influx of calcium into the cell and the ensuing cellular calcium response. Our experiments show that the addition of the putative specific Aβ channel blocker, NAHIS04, before exposing the cells to Aβ, eliminates the resulting cellular calcium response. In long time cell cultures, the addition of NAHIS04 to the culture medium also prevents the subsequent cell death that occurs after long exposure of cells to Aβ. The specificity of interaction of NAHIS04 with Aβ molecules, as shown in the artificial membrane experiments, and the elimination of other possible routes for the entry of calcium into the cells with nitrendipine, widely used to efficiently block voltage-dependent membrane calcium channels, ensure that NAHIS04 is specifically and effectively affecting the action of the calcium channels formed by Aβ. Therefore, our results provide strong support for the idea that the intracellular calcium increase observed when cells are exposed to Aβ is initiated by calcium fluxes across the cell membrane through newly formed Aβ channels.

We have suggested that the interaction between His derivative molecules that suppress Aβ cytotoxicity, such as NAHIS04 and the Aβ channels, may occur at the His residues of the Aβ molecule (*9*−*11*). This suggestion is supported by results of experiments in which His residues of the blocker were mutated (*9*, *10*) and experiments in which the reactive sites of the NAHIS04 molecules were removed by methylation (*11*). Additional support for this suggestion appears in a recent report that shows that substitutions of these His residues of the Aβ molecule affect peptide aggregation, metal binding, redox chemistry, and cell membrane interactions, factors that have previously been shown to modulate Aβ toxicity (*23*). There are three His residues in the Aβ molecule, which are located in the pore of previously proposed Aβ channel models (*6*). Although our latest generation of Aβ models (*8*) differs substantially from our original models (*6*), the same segment forms the pore. On the basis of these models, we predict that the principal binding site for a variety of channel blockers (inorganic multivalent cations Zn^{2+} and Al^{3+}, organic cationic drugs MRS2481 and MRS2485, and histidine-containing peptides, including NAHIS04) involves residues E11, H13, and H14 located at the C-terminal end of a pore-forming β-barrel. Recent findings suggest that the binding site for the Aβ channel blocker Zn^{2+} may not be specific to just this region of the Aβ molecule. Two nonamyloidogenic truncated amyloid-β fragment (Aβ11−42 and Aβ17−42) peptides were found recently to form ion channels in lipid membranes (*24*). The conductance of these channels was selectively inhibited by zinc, despite one of these Aβ fragments being truncated at the region containing the well-characterized Zn^{2+}-binding motif observed in different metalloproteases (*25*).

REFERENCES

1. Arispe, N., Rojas, E., and Pollard, H. B. (1993) Alzheimer disease amyloid β-protein forms calcium channels in bilayer membranes: Blockade by tromethamine and aluminum. *Proc. Natl. Acad. Sci. U.S.A. 90*, 567–571.
2. Kawahara, M., Arispe, N., Kuroda, Y., and Rojas, E. (1997) Alzheimer's disease amyloid β-protein forms Zn^{2+}-sensitive cation-selective channels across excited membrane patches from hypothalamic neurons. *Biophys. J. 73*, 67–75.
3. Arispe, N., Diaz, J., and Simakova, O. (2007) Aβ ion channels. Prospects for treating Alzheimer's disease with Aβ channel blockers. *Biochim. Biophys. Acta 1768*, 1952–1965.
4. Arispe, N., Pollard, H. B., and Rojas, E. (1994) The ability of Amyloid β-protein [AβP(1−40)] to form Ca^{2+} channels provides a mechanism for neuronal death in Alzheimer's disease. *Ann. N.Y. Acad. Sci. 747*, 256–266.

5. Kawahara, M. (2004) Disruption of calcium homeostasis in the pathogenesis of Alzheimer's disease and other conformational diseases. *Curr. Alzheimer Res. 1*, 87–95.
6. Durell, S. R., Guy, H. R., Arispe, N., Rojas, E., and Pollard, H. B. (1994) Theoretical models of the ion channel structure of amyloid-β-protein. *Biophys. J. 67*, 2137–2145.
7. Arispe, N., Pollard, H. B., and Rojas, E. (1996) Zn^{2+} interaction with Alzheimer amyloid β protein calcium channels. *Proc. Natl. Acad. Sci. U.S.A. 93*, 1710–1715.
8. Shafrir, Y., Durel, S. R., Arispe, N., and Guy, H. R. (2010) Models of Membrane-bound Alzheimer's Aβ Peptide Assemblies. *Proteins: Struct., Funct., Bioinf.* (in press).
9. Arispe, N. J. (2004) Architecture of the Alzheimer's AβP ion channel. *J. Membr. Biol. 197* (1), 33–48.
10. Diaz, J. C., Linnehan, J., Pollard, H., and Arispe, N. (2006) Histidines 13 and 14 in the Aβ sequence are targets for inhibition of Alzheimer's disease Aβ ion channel and cytotoxicity. *Biol. Res. 39*, 447–460.
11. Arispe, N., Diaz, J., and Flora, M. (2008) Efficiency of histidine-associating compounds for blocking the Alzheimer's Aβ channel activity and cytotoxicity. *Biophys. J. 95*, 4879–4889.
12. Simakova, O., and Arispe, N. (2006) Early and late cytotoxic effects of external application of the Alzheimer's Aβ result from the initial formation and function of ion channels. *Biochemistry 45*, 5907–5915.
13. Mattson, M. P., Cheng, B., Davis, D., Bryant, K., Lieberburg, I., and Rydel, R. E. (1992) β-Amyloid peptides destabilize calcium homeostasis and render human cortical neurons vulnerable to excitotoxicity. *J. Neurosci. 12* (2), 376–389.
14. Bhatia, R., Lin, H., and Lal, R. (2000) Fresh and globular amyloid β protein (1−42) induces rapid cellular degeneration: Evidence for AβP channel-mediated cellular toxicity. *FASEB J. 14* (9), 1233–1243.
15. Zhu, Y. J., Lin, H., and Lal, R. (2000) Fresh and nonfibrillar amyloid β protein(1−40) induces rapid cellular degeneration in aged human fibroblasts: Evidence for AβP-channel-mediated cellular toxicity. *FASEB J. 14* (9), 1244–1254.
16. Lin, H., Bhatia, R., and Lal, R. (2001) Amyloid β protein forms ion channels: Implications for Alzheimer's disease pathophysiology. *FASEB J. 15* (13), 2433–2444.
17. Kawahara, M., Kuroda, Y., Arispe, N., and Rojas, E. (2000) Alzheimer's β-amyloid, human islet amylin, and prion protein fragment evoke intracellular free calcium elevations by a common mechanism in a hypothalamic GnRH neuronal cell line. *J. Biol. Chem. 275* (19), 14077–14083.
18. Quist, A., Doudevski, I., Lin, H., Azimova, R., Ng, D., Frangione, B., Kagan, B., Ghiso, J., and Lal, R. (2005) Amyloid ion channels: A common structural link for protein-misfolding disease. *Proc. Natl. Acad. Sci. U.S.A. 102* (30), 10427–10432.
19. Diaz, J. C., Simakova, O., Jacobson, K. A., Arispe, N., and Pollard, H. B. (2009) Small molecule blockers of the Alzheimer Aβ calcium channel potently protect neurons from Aβ cytotoxicity. *Proc. Natl. Acad. Sci. U.S.A. 106* (9), 3348–3353.
20. Bezprozvanny, I., and Mattson, M. P. (2008) Neuronal calcium mishandling and the pathogenesis of Alzheimer's disease. *Trends Neurosci. 31* (9), 454–463.
21. Green, K. N., and LaFerla, F. M. (2008) Linking Calcium to Aβ and Alzheimer's Disease. *Neuron 59*, 190–194.
22. Demuro, A., Parker, I., and Stutzmann, G. E. (2010) Calcium Signaling and Amyloid Toxicity in Alzheimer's Disease. *J. Biol. Chem. 285* (17), 12463–12468.
23. Smith, D. G., Ciccotosto, G. D., Tew, D. J., Perez, K., Curtain, C. C., Boas, J. F., Masters, C. L., Cappai, R., and Barnham, K. J. (2010) Histidine 14 Modulates Membrane Binding and Neurotoxicity of the Alzheimer's Disease Amyloid-β Peptide. *J. Alzheimer's Dis. 19*, 1387–1400.
24. Jang, H. (2010) Truncated β-amyloid peptide channels provide an alternative mechanism for Alzheimer's disease and Down syndrome. *Proc. Natl. Acad. Sci. U.S.A. 107* (14), 6538–6543.
25. Perlman, R. K., and Rosner, M. R. (1994) Identification of zinc ligands of the insulin-degrading enzyme. *J. Biol. Chem. 269* (52), 33140–33145.